EXTENDED PDF FORMAT
SPONSORED BY

BIO-RAD

http://discover.bio-rad.com



Oceanic Rossby Waves Acting As a "Hay Rake" for Ecosystem Floating By-Products

Yves Dandonneau, *et al.*

Science **302**, 1548 (2003);
DOI: 10.1126/science.1090729

The following resources related to this article are available online at www.sciencemag.org (this information is current as of January 2, 2007):

A correction has been published for this article at:
http://www.sciencemag.org/cgi/content/full/303/5655/173a

Updated information and services, including high-resolution figures, can be found in the online version of this article at:
http://www.sciencemag.org/cgi/content/full/302/5650/1548

A list of selected additional articles on the Science Web sites **related to this article** can be found at:
http://www.sciencemag.org/cgi/content/full/302/5650/1548#related-content

This article **cites 2 articles**, 1 of which can be accessed for free:
http://www.sciencemag.org/cgi/content/full/302/5650/1548#otherarticles

This article has been **cited by** 11 article(s) on the ISI Web of Science.

This article has been **cited by** 3 articles hosted by HighWire Press; see:
http://www.sciencemag.org/cgi/content/full/302/5650/1548#otherarticles

This article appears in the following **subject collections**:
Oceanography
http://www.sciencemag.org/cgi/collection/oceans

Information about obtaining **reprints** of this article or about obtaining **permission to reproduce this article** in whole or in part can be found at:
http://www.sciencemag.org/help/about/permissions.dtl

Downloaded from www.sciencemag.org on January 2, 2007

Science (print ISSN 0036-8075; online ISSN 1095-9203) is published weekly, except the last week in December, by the American Association for the Advancement of Science, 1200 New York Avenue NW, Washington, DC 20005. Copyright c 2006 by the American Association for the Advancement of Science; all rights reserved. The title SCIENCE is a registered trademark of AAAS.

CORRECTED 9 JANUARY 2004; SEE LAST PAGE

ear charge density of the DNA-CNT hybrid relative to that of the DNA wrap alone, based on an image charge analysis for adjacent dielectrics (*20*). This fundamental difference in behavior provides ample differentiation between the binding strengths of metallic and semiconducting nanotubes to the anion exchange resin. Among semiconducting DNA-CNTs, there are two (nonexclusive) mechanisms that allow linear charge density to depend on tube diameter. First, because the polarizability of semiconducting nanotubes depends on diameter (*21*), the effective linear charge density is diameter-dependent. Second, the linear charge density of the DNA can change with tube diameter due to wrapping geometry changes. Together, these allow diameter-dependent separation of semiconducting tubes.

In summary, we have found that the attachment of ssDNA to a CNT is dependent on the specific DNA sequence and have shown that this can form the basis for a method for CNT diameter and type separation.

References and Notes

1. M. S. Dresselhaus, G. Dresselhaus, P. C. Eklund, *Science of Fullerenes and Carbon Nanotubes* (Academic Press, San Diego, CA, 1996).
2. R. Saito, G. Dresselhaus, M. S. Dresselhaus, *Physical Properties of Carbon Nanotubes* (Imperial College Press, London, 1998).
3. P. Avouris, *Acc. Chem. Res.* **35**, 1026 (2002).
4. S. Niyogi *et al.*, *Acc. Chem. Res.* **35**, 1105 (2002).
5. H. Dai, *Acc. Chem. Res.* **35**, 1035 (2002).
6. M. Zheng *et al.*, *Nature Mater.* **2**, 338 (2003).
7. D. Chattopadhyay, I. Galeska, F. A. Papadimitrakopoulos, *J. Am. Chem. Soc.* **125**, 3370 (2003).
8. R. Krupke, F. Hennrich, H. v. Lohneysen, M. M. Kappes, *Science* **301**, 344 (2003).
9. J. Liu *et al*, *Science* **280**, 1253 (1998).
10. D. Chattopadhyay, S. Lastella, S. Kim, F. Papadimitrakopoulos, *J. Am. Chem. Soc.* **124**, 728 (2002).
11. S. K. Doorn *et al.*, *J. Am. Chem. Soc.* **124**, 3169 (2002).
12. M. J. O'Connell *et al.*, *Science* **297**, 593 (2002).
13. S. M. Bachilo *et al.*, *Science* **298**, 2361 (2002).
14. M. S. Strano *et al.*, *Nano Lett.* **3**, 1091 (2003).
15. J. L. Sauvajol *et al.*, *Carbon* **40**, 1697 (2002).
16. J. R. Williamson, *Annu. Rev. Biophys. Biomol. Struct.* **23**, 703 (1994).
17. T. C. Marsh, J. Vesenka, E. Henderson, *Nucleic Acids Res.* **23**, 696 (1995).
18. G. S. Manning, *Q. Rev. Biophys.* **2**, 179 (1978).
19. G. S. Manning, *Biophys. Chem.* **101-102**, 461 (2002).
20. J. D. Jackson, *Classical Electrodynamics* (John Wiley & Sons, New York, ed. 3, 1999).
21. L. X. Benedict, S. G. Louie, M. L. Cohen, *Phys. Rev. B* **52**, 8541 (1995).

22. This work comes from the Molecular Electronics group at DuPont CR&D. The DuPont group developed DNA-CNT hybrid materials and CNT separation strategy. The UIUC group and the MIT group independently conducted Raman spectroscopy analysis on fractionated CNT samples. A.P.S. acknowledges partial support from the Brazilian agency CNPq. M.S. acknowledges fundings from the National Science Foundation (grant CTS-0330350), the School of Chemical Sciences of the UIUC, and U.S. Department of Energy (award no. DEFG02-91ER45439).

Supporting Online Material

www.sciencemag.org/cgi/content/full/302/5650/1545/DC1
SOM Text
Table S1
Figs. S1 to S7
References

25 September 2003; accepted 20 October 2003

Oceanic Rossby Waves Acting As a "Hay Rake" for Ecosystem Floating By-Products

Yves Dandonneau,[1]* Andres Vega,[2] Hubert Loisel,[3] Yves du Penhoat,[2] Christophe Menkes[1]

Recent satellite observations of Rossby waves and chlorophyll anomalies propagating in subtropical gyres have suggested that wave-induced upwelling could stimulate photosynthesis. Instead, we show that chlorophyll maxima are located in abnormally warm water, in Rossby wave–induced convergences. This excludes inputs of nutrients from deeper water. We argue that the sea color anomalies are not caused by chlorophyll but by floating particles evolved from the ecosystem and accumulated by Rossby waves, acting as "marine hay rakes," in convergence zones. Such processes may be determinant for the distribution of living organisms in oligotrophic areas.

Subtropical anticyclonic gyres occur in about 40% of the world's oceans and have very low nutrient and chlorophyll levels as well as permanently deep pycnoclines and nutriclines. In these oligotrophic areas, respiration balances and sometimes exceeds photosynthesis (*1*). Primary production is mostly supported by the regeneration of nutrients by the microbial loop, whereas export production remains low all year. Export production estimates based on seasonal geochemical budgets, though low, are not entirely accounted for by the mean upwelling of nutrients to the photic layer (*2*, *3*). Thus, it has been suggested that eddy-induced nutrient pumping to the photic layer (*3*) may account for the remainder of export production.

Recently, large-scale propagations of Rossby waves (RWs) from sea level and concurrent ocean color signals have been observed in all subtropical gyres. Nutrient pumping into the photic layer has been proposed as the mechanism by which RWs could increase chlorophyll concentration in these oligotrophic areas (*4*, *5*). Thus, RWs would act like a "rototiller" by lifting nutrients continuously to the photic layer as they propagate (*6*), accounting for some of the missing production in the subtropical gyres. However, the coupling between the dynamics and chlorophyll anomalies has not been elucidated. Using satellite data, we examine here the relations between RWs and chlorophyll concentration in the south Pacific subtropical gyre. We focus on the area 16°S to 22°S, 120°W to 80°W, where RWs have a marked signature.

A typical case is shown for May 2000 (Fig. 1). Filtered fields of sea-level anomalies (SLAs) induced by RWs (*7*) can be interpreted at first order as inverse variations of thermocline depth (*8*). Consequently, more complex mechanisms such as other baroclinic modes (*9*) are neglected. Then, crests and troughs indicate anticyclonic and cyclonic eddies (Fig. 1B). Divergence or convergence of quasi geostrophic surface current has been derived from SLAs (*10*). It corresponds to regions of upwelling or downwelling, respectively (Fig. 1A), spatially shifted from SLA troughs and crests (Fig. 1B). As expected, minima in sea surface temperature anomaly (SSTA) (*11*) correspond to upwelling and maxima, to downwelling (Fig. 1C). Surprisingly, positive chlorophyll anomalies (ChlA) (*12*) are co-located with convergence and positive SSTA (Fig. 1D). This is unexpected, because increased surface phytoplankton concentration is generally related with upwelling of cold and nutrient-rich water. Nutrient inputs in these convergence areas should be less than anywhere else (*13*), and thus only delayed use by phytoplankton of horizontally advected nutrients might explain chlorophyll maxima in these places. However, the time for surface water to drift from upwelling to downwelling patches (typically one month) is longer than needed by the phytoplankton to use such small amounts of nutrients. Hence, lags between nutrient inputs and their utilization cannot explain that positive ChlAs are located in convergences.

[1]IRD, IPSL/Laboratoire d'Océanographie Dynamique et de Climatologie, 75252 Paris 05, France. [2]IRD, Laboratoire d'Etudes en Géophysique et Océanographie Spatiale, Toulouse, France. [3]MREN- Université du Littoral - Côte d'Opale, UMR 8013, Wimereux, France.

*To whom correspondence should be addressed. E-mail: yd@lodyc.jussieu.fr

Downloaded from www.sciencemag.org on January 2, 2007

The relations observed in May 2000 (Fig. 1) can be extended all along RW westward propagations in the 15°S to 22°S band (Fig. 2). RW-related anomalies are clearly observed in all diagrams. Again, positive ChlA and SSTA are located in convergence regions. All of this strongly suggests that the vertical motions induced by RWs are not the dominant mechanisms at work to explain the location of ocean-color signals propagating along with RWs.

If ChlAs are not caused by the usual mechanisms in these RW systems, it may be that they are not really chlorophyll anomalies. Then, we have to consider a possible artifact in the determination of chlorophyll from ocean color in the studied region. The ocean color algorithms (*14*) estimate chlorophyll concentration using the 443 (blue) to 550 nm (green) reflectances ratio (B/G) which decreases with increasing chlorophyll concentration. The retrieval of chlorophyll from B/G assumes that the various absorbing and backscattering organic constituents of seawater are in constant proportions. This assumption is generally reasonable, as attested by the extensive use of ocean color data in many studies, but may sometimes lead to biases, even in the open ocean. A bias in SeaWiFS (Sea-viewing Wide Field-of-view Sensor) estimates (up to 100 % greater than chlorophyll measured in situ) in the Mediterranean Sea has thus been attributed to nonalgal particles in excess, compared with standard oceanic waters with the same chlorophyll content (*15*). This bias was observed in low-chlorophyll waters such as those investigated here. Indeed, nonalgal particles in excess tend to decrease B/G. Likewise, B/G decreases when blue-absorbing dissolved colored organic matter is abundant (*16*). Therefore, it must be kept in mind that B/G, used by all ocean color sensors, also varies with nonchlorophyll-containing substances. The reported small deviations may be nothing but the result of biases in the retrieval of chlorophyll from space. How these biases are co-located with the convergence patterns remains to be explained.

We assumed that low-density nonchlorophyllous metabolites and detritus, henceforth mentioned as floating particulate organic carbon (fPOC), are generated by the ecosystem and accumulate near the sea surface (*17*). RW-induced transport of fPOC tends to remove it from divergences and accumulate it in convergences, where it remains near the surface while seawater subducts. These substances modify the transfer of light in the sea (*18*, *19*) and should be detected by SeaWiFS as chlorophyll anomalies. To test this hypothesis, we simulate the convergent vertical circulation across RWs, as well as the production and advection of fPOC (*20*) (Fig. 3B). The model transfers fPOC from the upwelling to the subduction areas where it is trapped at the sea surface, generating a strong horizontal gradient (Fig. 3B). Marine reflectances at SeaWiFS wavelengths are then simulated using a radiative transfer model in which only fPOC varies (*21*). Finally, apparent chlorophyll concentration is computed using the SeaWiFS algorithm (*14*) (Fig. 3A). In spite of constant chlorophyll concentration in the model, the apparent chlorophyll variability (0.04 mg m^{-3}) caused by fPOC and affecting SeaWiFS detection is coherent with the observations. Model sensitivity tests indicate that fPOC concentration near the surface increases with floatability and decreases with decay rate. fPOC production, which was set to 1% of primary production in the model, may be given greater values: sediment traps

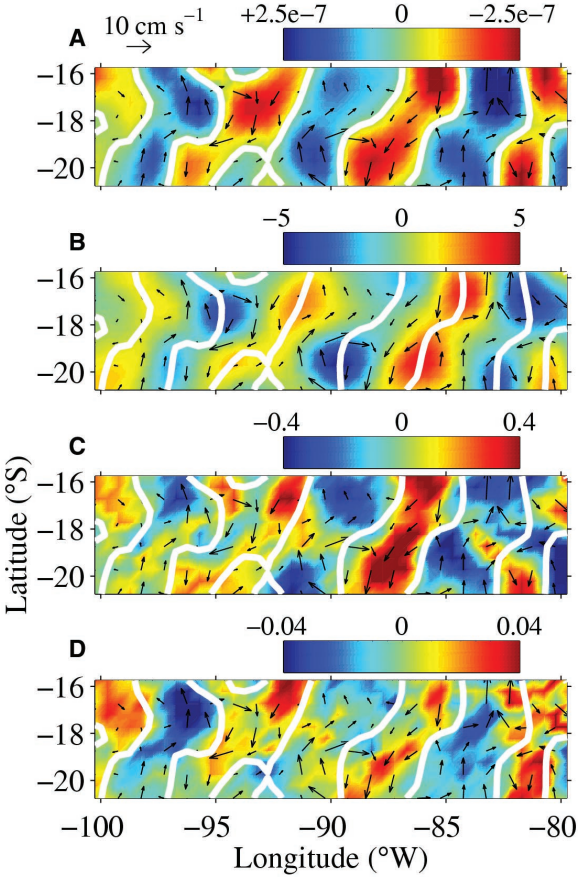


Fig. 1. May 2000 maps of monthly bandpassed satellite observations in the South Pacific subtropical gyre. (**A**) Convergence (= negative divergence), (**B**) SLAs, (**C**) SSTAs and (**D**) ChlAs. Black arrows are geostrophic currents (*10*). Red, positive convergences, SLAs, SSTAs, and ChlAs; blue, negative convergences, SLAs, SSTAs, and ChlAs. White contours of the convergence field are replicated on all maps.

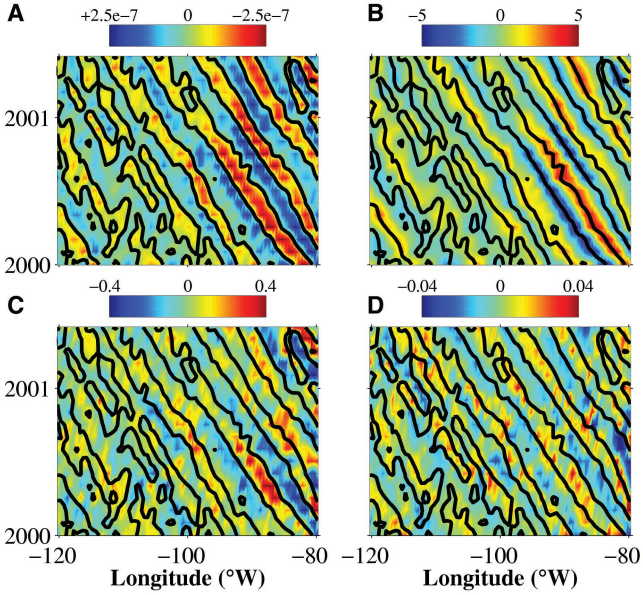


Fig. 2. Longitude-time diagrams of satellite observations in the South Pacific subtropical gyre at 20°S. (**A**) Convergence, (**B**) SLAs, (**C**) SSTAs, and (**D**) ChlAs. Red, positive values; blue, negative values. Black contours of the convergence field are replicated on all panels. For sake of clarity, only the area between 80°W and 120°W, and from January 2000 to June 2001 is represented.

Downloaded from www.sciencemag.org on January 2, 2007

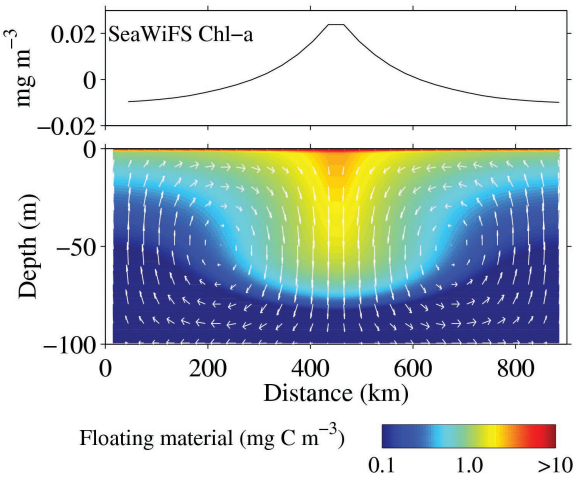


Fig. 3. Numerical simulation of the dynamics of floating particles that may generate satellite-detected chlorophyll-like anomalies. (**Bottom**) Convergence of fPOC. Circulation in the vertical plane (adjusted to the observed RW dynamics) concentrates fPOC at the convergence of surface current, where its interaction with light results in lower B/G. This is "seen" by SeaWiFS algorithm (**top**) as chlorophyll concentration higher than in the divergence areas on both sides.

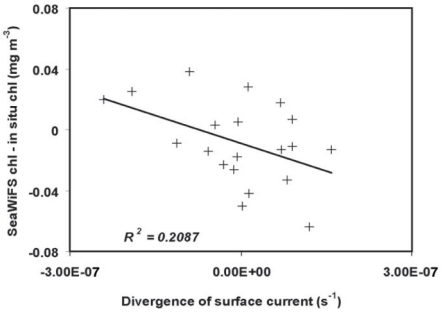


Fig. 4. Relation between divergence of the surface current and the difference of SeaWiFS Chl minus in situ chlorophyll. In situ chlorophyll were collected during the GeP&CO (Geochemistry, Phytoplankton, and Color of the Ocean) program, in the area 15°S to 25°S, 150°W to 170°W. The difference is computed using daily level 3 SeaWiFS chlorophyll estimates with in situ data. Only collocated data separated by *dt* (in hours) and *dl* (in km), such that *dt* + 0.5 *dl* is less than 10, are considered. This criterion was adopted to select enough data points (only one GeP&CO measurement was exactly co-located with a SeaWiFS estimate). Influence of this arbitrary choice on the final result is small. Divergence is computed using nonfiltered weekly altimetry data (*7*, *10*), interpolated at the date and location of the chlorophyll measurements.

oriented upward and downward have measured an upward flux of particles as high as two-thirds of the downward flux (*17*). Thus, if production exported to depth is 6% of primary production, a typical value in tropical oligotrophic waters (*22*), then up to 4% of primary production may result in fPOC, leading to an increase four times higher than in our simulation. Presence of gas bubbles, coated with organic film or trapped in fPOC, would also increase the light backscattering coefficient and cause larger bias (*23*). This simple model, forced by realistic values, provides a framework by which to understand how fPOC can be seen as apparent chlorophyll excess at the RW convergences. However, we need field evidence of particles concentration at the sea surface by this process.

If our hypothesis is valid, then SeaWiFS estimates would be higher than in situ chlorophyll, especially in convergences. Field data to demonstrate such overestimation are scarce. However, we could test it using the difference between SeaWiFS chlorophyll estimates and collocated in situ chlorophyll data from 12 cruises from 1999 to 2002 (www.lodyc.jussieu.fr/gepco/). Each of these cruises includes seven to nine determinations (chlorophyll a + divinyl chlorophyll a) between 18°S and 25°S on the shipping route from Tahiti to Auckland. Only 20 of ~100 measurements were co-located with SeaWiFS daily level 3 data (Fig. 4). Although these data were collected farther west than 120°W, in an area where RW energy tends to dissipate (*8*), they indeed show an inverse relation ($r^2 = 0.21$, significant at the 95% confidence level) between local divergence and the difference SeaWiFS minus in situ chlorophyll.

An additional argument is provided by wind data: Under strong wind conditions, fPOC should be dispersed in the mixed layer and not be seen from satellite, in the same way that slicks generated by Langmuir circulation cells, rich in floating material (*24*), are dispersed when wind speed exceeds 6 m s^{-1} (*25*). Fields of convergence and ChlAs such as those presented in Fig. 1 are positively correlated. We computed a time series of this correlation from October 1997 to March 2001. It was lowest, around 0.2, in 1998 and until early 1999, during a strong La Niña episode when average wind speed (*26*) exceeded 6 m s^{-1}. Later, wind speed decreased and correlation improved, around 0.35. Low correlations are also found in austral winter and spring, when wind speed increases. Conversely, high correlations characterize low-wind periods, such as May to June 1999 and December 1999 to January 2000. Though direct observations of particles concentration in convergences are still lacking, the obvious effect of average wind speed, together with the higher values of SeaWiFS minus in situ chlorophyll found in convergences, support our hypothesis.

There is little doubt that the sea surface is a layer in which many substances tend to congregate (*17*, *24*). However, we know very little about this process. Oceanographic cruises usually skip the upper 2 or 3 meters due to practical sampling constraints. Therefore, it is presently not possible to give an exact picture of fPOC. It can consist of flocculated colloids, or detritus, in which bacterial activity has evolved bubbles. The neuston is adapted to stay just below the surface and to resist downward water motion. Some phytoplankton species adjust their floatability according to their nutrients content or light requirements. This is the case for some *Rhizosolenia sp*. diatoms (*27*) that may make "lines in the sea" in nutrient-rich environments (*28*); however, this process is not likely to occur in the oligotrophic South Pacific subtropical gyre. Control of floatability by gas bubbles, such as in some picoplanktonic cyanobacteria (*29*), might more likely play a role here. A two-step mechanism may also act: after maturation time, accumulation of organic material at the sea surface favors the growth of bacteria, and hence nutrient regeneration (*19*), and, in turn, phytoplankton growth and chlorophyll increase.

Processes that do not need the supply of new nutrients are seldom proposed to explain the biological variability in the oceans. We have shown that the image of a RW-powered "rototiller" eroding the nutrient-rich deep waters (*6*) does not apply in the South Pacific subtropical gyre. A "hay rake" (another agricultural machine) that concentrates in restricted areas the organic material produced uniformly around by the marine ecosystem, provides a better representation of the processes at work. This implies a decoupling of biogenic particles from water circulation, because it is based on substances that float. The JGOFS (Joint Global Ocean Flux Study) decade has been devoted to the downward flux of particles. Here, we show that a flux of floating particles can lead to increased concentrations of material in convergence areas, including fronts and subduction zones. This is of interest because (i) it may modify ocean color and be detected from satellites, (ii) it may affect the gas exchange through the air-sea interface, and (iii) it may be a source of food for fish that live near the surface. Further, because satellite-detected sea color is often used to validate biogeochemical models, adding floating material in these models may improve the simulations in places where convergence and fronts occur.

References and Notes

1. L. Legendre, *J. Geophys. Res.* **103**, 2897 (1998)
2. J. R. Christian, M. R. Lewis, D. M. Karl, *J. Geophys. Res.* **102**, 15667 (1997).
3. D. J. McGillicuddy Jr. *et al.*, *Global Biogeochem. Cycles* **17**, 10.1029/2002GB001987 (2003).

Downloaded from www.sciencemag.org on January 2, 2007

4. B. M. Uz, J. A. Yoder, V. Osychny, *Nature* **409**, 597 (2001).
5. P. Cipollini, D. Cromwell, P. G. Challenor, S. Raffaglio *Geophys. Res. Lett.*, **28**, 323 (2001).
6. D. A. Siegel, *Nature* **409**, 605 (2001).
7. SLAs from the combined TOPEX/Poseidon and ERS altimeters are produced by the CLS (Collecte Localisation Satellites) Space Oceanography Division (*30*). Fields from September 1997 to June 2001 have been interpolated on a 0.25° by 0.25° grid. Several interpolation techniques were applied, giving no relevant differences, and linear interpolation was adopted. Altimeter data were bandpass filtered to extract the signal at observed RW wavelengths and periods (300 km to 5000 km, and 3 months to 46 months). The filter, a two-dimensional (2D) finite impulse response filter, was applied on longitude-time diagrams (*5*). Harmonic fit was used to remove the annual cycle of the monthly series, followed by a zonal detrending of the residuals.
8. A. Vega, Y. du Penhoat, B. Dewitte, O. Pizarro, *Geophys. Res. Lett.* **30**, 10.1029/2002GL015886 (2003).
9. J. D. McNeil *et al.*, *J. Geophys. Res.* **104** , 15537, 1999.
10. Zonal (u) and meridional (v) currents are computed from SLA as $u = -(g/f)\ \partial(SLA)/\partial y$ and $v = (g/f)\ \partial(SLA)/\partial x$, where x and y are the zonal and meridional coordinates, g is gravity, $f = f_0 + \beta y$ is the leading part of the variation of the Coriolis parameter, $f_0 = 4.97\ 10^{-5}\ s^{-1}$ is the Coriolis parameter estimated at 20°S, and $\beta = 2.27\ 10^{-11}\ s^{-1}\ m^{-1}$ is the meridional derivative of f . Given the continuity equation, and the first baroclinic mode assumption, divergence or convergence $div = \partial u/\partial x + \partial v/\partial y = -\beta\ v/f_0$ of the horizontal flow is compensated by upwelling or downwelling, respectively, at the thermocline depth (*31*).
11. SST from the NASA-NASDA TRMM Microwave Imager (TMI) is provided by Remote Sensing Systems, interpolated and filtered in the same way as altimetry data.
12. Ocean color data are from the SeaWiFS Global Area Coverage (GAC) level 3 Standard Mapped Image data from NASA-GSFC DAAC (monthly composites), interpolated and filtered in the same way as altimetry data.
13. S. Neuer *et al.*, *Geophys. Res. Lett.* **29**, 10.1029/2002GL015393 (2002).
14. J. E. O'Reilly *et al.*, *J. Geophys. Res.* **103**, 24937 (1998).
15. H. Claustre *et al.*, *Geophys. Res. Lett.* **29**, 10.1029/2001GL014056 (2002).
16. K. L. Carder, R. G. Steward, G. R. Harvey, P. B. Ortner, *Limnol. Oceanogr.* **34**, 68 (1989).
17. K. L. Smith, P. M. Williams, E. R. M. Druffel, *Nature* **337**, 724 (1989).
18. D. A. Siegel, A. F. Michaels, *Deep-Sea Res. II* **43**, 321 (1996).
19. J. J. Cullen, M. R. Lewis, *J. Geophys. Res.* **100**, 13255 (1995).
20. The 2D (longitude, depth) circulation of the conceptual model is calculated by imposing a stream function giving surface current values peaking to 10 cm s^{-1} in agreement with the sea level–derived currents. It is limited to the top 100 m, i.e., the average euphotic depth and mixed layer in the south tropical Pacific, and its zonal extension of 900 km represents a typical RW zonal extension. This model simulates the production of fPOC and its accumulation at RW convergences, assuming constant biogeochemical conditions in the vertical. Chlorophyll concentration is set to 0.08 mg m^{-3}, and particulate organic carbon (POC) is set to 28 mg m^{-3}, as reported for this area (*32*). Net primary production decreases exponentially with depth as with light, amounting to an integrated value of 0.3 g C m^{-2} day^{-1}, typical of the subtropical gyres. Production of fPOC is set to 1% of net primary production, and this material is given an ascending speed equal to 1 m d^{-1}. One-tenth of fPOC in the upper 1 meter is destroyed each day, simulating its natural decay by photodegradation or grazing. With such source and sink, the equilibrium for fPOC is 60 mg C m^{-2} in the water column. This is a small addition to the system, as it represents only 2% of the POC estimated at 150°W, 16°S (*32*).
21. The Hydrolight (*33*) simulations were carried out for an infinitely deep ocean with a nearly flat sea surface and a sun in a black sky, and they used standard particulate volume scattering phase function (*34*) and absorption and scattering coefficients for pure sea water. The scattering coefficient by particles is parameterized as a function of total POC, with total POC = 28.0 + fPOC. The wavelength (λ)-dependent absorption coefficient by particles is assumed to be the sum of the absorption by phytoplankton, $a\Phi$, and another term, aPOC, representing the contribution of POC in the absorption process. $a\Phi(\lambda)$ is calculated as a function of chlorophyll (*35*), and aPOC(λ) is equal to aPOC(440) exp[–0.011 (λ – 440)], where the dependency of aPOC(440) on POC is the same as for nonalgal particles (*36*).
22. A. K. Aufdenkampe *et al.*, *Global Biogeochem. Cycles* **15**, 101 (2001).
23. X. Zhang, M. R. Lewis, B. Johnson, *Appl. Opt.* **37**, 6525 (1998).
24. L. R. Haury, C. L. Fey, E. Shulenberger, *Deep-Sea Res. I* **41**, 1191 (1994).
25. J. C. Romano, *Deep-Sea Res. I* **43**, 411 (1996).
26. Weekly 1° by 1° gridded wind fields from the ERS-1/2 scatterometer were provided by CERSAT (IFREMER).
27. T. A. Villareal, S. Woods, J. K. Moore, K. Culver-Rymsza, *J. Plankton Res.* **18**, 1103 (1996).
28. J. A. Yoder, S. G. Ackleson, R. T. Barber, P. Flament, *Nature* **371**, 689 (1994).
29. B. B. Wallace, D. P. Hamilton, *Limnol. Oceanogr.* **44**, 273 (1999).
30. N. Ducet, P. Y. Le Traon, G. Reverdin, *J. Geophys. Res.* **105**, 19477 (2000).
31. A. E. Gill, *Atmosphere Ocean Dynamics* (Academic Press, New York 1982).
32. H. Claustre *et al.*, *J. Geophys. Res.* **104**, 3401 (1999).
33. C. D. Mobley, *Hydrolight 4.0 User's Guide* (Sequoia Scientific, Mercer Island, WA, 1998).
34. T. J. Petzold, Tech. Rep. Ref. 72-78 (Scripps Institution of Oceanography, San Diego, CA, 1972).
35. A. Bricaud, M. Babin, A. Morel, H. Claustre, *J. Geophys. Res.* **100**, 13321 (1995).
36. A. Bricaud, A. Morel, M. Babin, K. Allali, H. Claustre, *J. Geophys. Res.* **103**, 31033 (1998).

37. The Hydrolight simulations of marine reflectances at SeaWiFS wavelengths have been done at Scripps Institution of Oceanography, USCD, by J. Piskozub. We acknowledge discussions with J. C. Romano and G. Gorsky. A. Vega benefited from a grant from IRD.

25 August 2003; accepted 24 October 2003

A Transient Rise in Tropical Sea Surface Temperature During the Paleocene-Eocene Thermal Maximum

James C. Zachos,[1]* Michael W. Wara,[1] Steven Bohaty,[1] Margaret L. Delaney,[1] Maria Rose Petrizzo,[2] Amanda Brill,[3] Timothy J. Bralower,[4] Isabella Premoli-Silva[2]

The Paleocene-Eocene Thermal Maximum (PETM) has been attributed to a rapid rise in greenhouse gas levels. If so, warming should have occurred at all latitudes, although amplified toward the poles. Existing records reveal an increase in high-latitude sea surface temperatures (SSTs) (8° to 10°C) and in bottom water temperatures (4° to 5°C). To date, however, the character of the tropical SST response during this event remains unconstrained. Here we address this deficiency by using paired oxygen isotope and minor element (magnesium/calcium) ratios of planktonic foraminifera from a tropical Pacific core to estimate changes in SST. Using mixed-layer foraminifera, we found that the combined proxies imply a 4° to 5°C rise in Pacific SST during the PETM. These results would necessitate a rise in atmospheric pCO_2 to levels three to four times as high as those estimated for the late Paleocene.

The Paleocene-Eocene Thermal Maximum [55 million years ago (Ma)] was accompanied by a number of environmental perturbations, including mass extinction of benthic foraminifera (*1*), widespread appearance and proliferation of exotic plankton in the open and coastal oceans (*2–5*), shifts in precipitation patterns and intensity (*6*), and migration and dispersal of terrestrial mammals (*7*). These perturbations are attributed to a global warming of unusual magnitude (*8–10*). That this warming was greenhouse gas–induced is supported by two independent lines of evidence: a >2.5‰ negative carbon isotope excursion (CIE) of the entire global exogenic carbon pool and a pronounced deep-sea carbonate dissolution horizon. Both are consistent with injections of a large mass of ^{12}C-enriched carbon into the ocean/atmosphere (*11*). The primary source of this carbon has been postulated to be the dissociation of methane hydrate (*12*).

In theory, a substantial increase in atmospheric CO_2 and/or CH_4 levels as posited for the PETM should have induced warming at all latitudes, with SST increases amplified toward the poles. This pattern of warming is a robust feature of greenhouse simulations that use coupled ocean-atmosphere models with a strong ice-albedo feedback (*13*). Simulations with a fixed ice-albedo feedback also exhibit polar amplification, but to a lesser extent (*14*). In this regard, the PETM pro-

[1]Earth and Ocean Sciences Departments, University of California, Santa Cruz, CA 95064, USA. [2]Dipartimento di Scienze della Terra "Ardito Desio," Universita' degli Studi di Milano, via Mangiagalli 34, Milano 20133, Italy. [3]Department of Geological Sciences, University of North Carolina, Chapel Hill, NC 27599, USA. [4]Department of Geosciences, Pennsylvania State University, University Park, PA 16802, USA.

*To whom correspondence should be addressed. E-mail: jzachos@es.ucsc.edu

Downloaded from www.sciencemag.org on January 2, 2007

ERRATUM

post date 9 January 2004

REPORTS: "Oceanic Rossby waves acting as a 'hay rake' for ecosystem floating by-products" by Y. Dandonneau *et al.* (28 Nov. 2003, p. 1548). There were errors in three of the figures. The ranges indicated in Fig. 1A and Fig. 2A should read "+2.5e-8" to "–2.5e-8," and the range indicated on the *x* axis in Fig. 4 should read "–3.00E-08" to "3.00E-08."

Downloaded from www.sciencemag.org on January 2, 2007